

PL-TR-97-2010

# **PASP PLUS TRANSIENT PULSE MONITOR (TPM) - DATA ANALYSIS AND INTERPRETATION REPORT**

Richard C. Adamo  
C. Max Hammond  
David R. Dana

SRI International  
333 Ravenswood Avenue  
Menlo Park, CA 94025

September 1996

Final Report  
26 April 1993-30 April 1996

APPROVED FOR PUBLIC RELEASE; DISTRIBUTION UNLIMITED

**DTIC QUALITY INSPECTED 4**




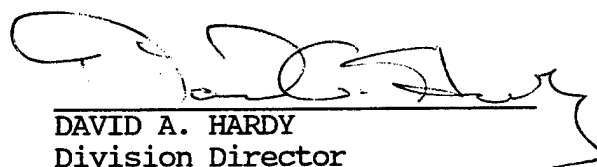
**PHILLIPS LABORATORY  
DIRECTORATE OF GEOPHYSICS  
AIR FORCE MATERIEL COMMAND  
HANSCOM AIR FORCE BASE, MA 01731-3010**

19970520 173

This technical report has been reviewed and is approved for publication.

  
MARK D. CONFER, Major USAF  
Contract Manager

  
MARK D. CONFER, Major USAF  
Branch Chief

  
DAVID A. HARDY  
Division Director

This report has been reviewed by the ESC Public Affairs Office (PA) and is releasable to the National Technical Information Service (NTIS).

Qualified requestors may obtain additional copies from the Defense Technical Information Center (DTIC). All others should apply to the National Technical Information Service (NTIS).

If your address has changed, or if you wish to be removed from the mailing list, or if the addressee is no longer employed by your organization, please notify PL/IM, 29 Randolph Road, Hanscom AFB, MA 01731-3010. This will assist us in maintaining a current mailing list.

Do not return copies of this report unless contractual obligations or notices on a specific document require that it be returned.

**REPORT DOCUMENTATION PAGE**Form Approved  
OMB No. 0704-0188

Public reporting burden for this collection of information is estimated to average 1 hour per response, including the time for reviewing instructions, searching existing data sources, gathering and maintaining the data needed, and completing and reviewing the collection of information. Send comments regarding this burden estimate or any other aspect of this collection of information, including suggestions for reducing this burden, to Washington Headquarters Services, Directorate for Information Operations and Reports, 1215 Jefferson Davis Highway, Suite 1204, Arlington, VA 22202-4302, and to the Office of Management and Budget, Paperwork Reduction Project (0704-0188), Washington, DC 20503.

1. AGENCY USE ONLY (Leave Blank)		2. REPORT DATE September 1996		3. REPORT TYPE AND DATES COVERED Final—04/26/93 to 04/30/96	
4. TITLE AND SUBTITLE PASP Plus Transient Pulse Monitor (TPM) - DATA ANALYSIS AND INTERPRETATION REPORT				5. FUNDING NUMBERS PE 63410F PR 2822 TA GC WU SR Contract F19628-93-K-0014	
6. AUTHOR(S) Richard C. Adamo, C. Max Hammond, and David R. Dana					
7. PERFORMING ORGANIZATION NAME(S) AND ADDRESS(ES) SRI International 333 Ravenswood Avenue Menlo Park, CA 94025				8. PERFORMING ORGANIZATION REPORT NUMBER SRI Project 4651	
9. SPONSORING/MONITORING AGENCY NAME(S) AND ADDRESS(ES) Phillips Laboratory 29 Randolph Road Hanscom AFB, MA 01731-3010 Contract Manager: Major Mark Confer/GPSG				10. SPONSORING/MONITORING AGENCY REPORT NUMBER PL-TR-97-2010	
11. SUPPLEMENTARY NOTES					
12a. DISTRIBUTION/AVAILABILITY STATEMENT Approved for public release; distribution unlimited.				12b. DISTRIBUTION CODE	
13. ABSTRACT (Maximum 200 words) The Transient Pulse Monitor (TPM), part of the PASP Plus experiment aboard the APEX spacecraft, is designed to detect and characterize electromagnetic transient signals produced by electrostatic discharges on the solar array test modules. This report describes the results of the TPM post-mission data analyses performed for periods when the various test arrays were biased negatively with respect to the spacecraft. The report includes a developed "filter" algorithm for distinguishing between actual array discharges and electrical transients produced by other onboard sources, a discussion of the probabilities and characteristics of discharges (based on the "filter" algorithm) as functions of bias voltages and plasma densities, the results of efforts to determine more precise discharge locations, and a brief description of the TPM instrument.					
14. SUBJECT TERMS Transient Pulse Monitor (TPM), arc pulse parameter measurements, high-voltage arc discharge characterization				15. NUMBER OF PAGES 26	
				16. PRICE CODE	
17. SECURITY CLASSIFICATION OF REPORT UNCLASSIFIED	18. SECURITY CLASSIFICATION OF THIS PAGE UNCLASSIFIED	19. SECURITY CLASSIFICATION OF ABSTRACT UNCLASSIFIED	20. LIMITATION OF ABSTRACT SAR		

## CONTENTS

<b>ILLUSTRATIONS.....</b>	<b>iv</b>
<b>1 INTRODUCTION.....</b>	<b>1</b>
1.1 Background.....	1
1.2 Scope of this Report.....	1
<b>2 DATA ANALYSIS AND INTERPRETATION.....</b>	<b>2</b>
2.1 Development of an Array-Discharge Filter Algorithm.....	2
2.2 Effect of the Local Environment on Discharges.....	7
2.3 Location of Discharges .....	14
2.4 Summary .....	18
<b>3 REFERENCES.....</b>	<b>19</b>
<b>APPENDIX—TPM HARDWARE DESCRIPTION.....</b>	<b>21</b>

## ILLUSTRATIONS

1	Pulse integral vs. positive amplitude measured by the four TPM detectors for all times from 94215 to 94309 when biasing was active .....	4
2	Similar to Figure 1, except the data have been restricted to intervals when none of the arrays was biased.....	4
3	Pulse integral vs. positive amplitude measured by sensor 1 for four different ranges of negative biasing .....	6
4	Trajectory of the spacecraft for two orbits in magnetic coordinates.....	8
5	Probability of discharge vs. bias voltage during noneclipse intervals for the modules listed in Table 1.....	10
6	Probability of discharge for Module 2 at various negative bias voltages and electron densities as measured by the Langmuir probe .....	12
7	Positive amplitude and integral vs. bias voltage for Module 2 during noneclipse intervals.....	13
8	Top view of the spacecraft where the position of the biased module and the location of the four TPM sensors are shown.....	16
9	Similar to Figure 8, except both the amplitude and integral were used to find the predicted location of the discharge.....	16
10	Same as Figure 9, except for intervals when Module 3 was negatively biased.....	17
11	Similar to Figure 8, except the initial amplitude of the signal was treated as a free parameter during the minimization routine to find the predicted location of the discharge .....	17

# **1 INTRODUCTION**

## **1.1 BACKGROUND**

On August 3, 1994, the Photovoltaic Array Space Power Plus Diagnostics (PASP Plus) experiment was launched aboard the Advanced Photovoltaic and Electronics Experiments (APEX) spacecraft by a standard Pegasus rocket released from a B-52 aircraft into a 70° inclination, 363 km × 2550 km orbit.

The objectives of the PASP Plus experiment (Guidice and Ray, 1996) were to

- Measure the plasma “leakage” current for different kinds of solar arrays subjected to positive biasing levels up to +500V
- Measure the arcing parameters for the different kinds of arrays subjected to negative biasing levels up to -500V
- Measure the long-term deterioration in the power output of arrays using different solar-cell materials when exposed to space radiation.

By August 1995, PASP Plus had collected an order of magnitude more data about environmental interactions on solar arrays than all previous space-borne photovoltaic experiments combined.

The Transient Pulse Monitor (TPM), built by SRI International under a previous contract (Dana, 1991), was the primary diagnostic instrument responsible for characterizing solar array arcs under negative biasing conditions, as required by the second objective in the bullet list above.

## **1.2 SCOPE OF THIS REPORT**

This report describes the results of TPM mission data analyses. In Section 2.1, we discuss the development of a filter to restrict the data to those pulses that are the result of real discharges rather than pulses due to normal electrical noise associated with the spacecraft. We show that discharges chosen by this filter behave as one might expect: the pulses become more numerous and larger when the arrays are biased at large negative voltages.

Additionally, in Section 2.2, we examine more quantitatively than in Section 2.1 the effect of bias voltage on the size of the discharge pulse, and the probability of discharges occurring under various bias voltages and plasma conditions.

We then show in Section 2.3 that the location of discharges may be determined in some instances if multiple TPM sensors record the signal. In general, however, the technique is not totally successful and possible explanations are discussed.

For completeness, the Appendix contains a brief description of the TPM hardware.

## **2 DATA ANALYSIS AND INTERPRETATION**

### **2.1 DEVELOPMENT OF AN ARRAY-DISCHARGE FILTER ALGORITHM**

As described in the Appendix, the TPM characterizes transient input signals in terms of the peak value of the amplitude, the derivative, and the integral of each pulse. It is important to note that not every event recorded by the TPM is the result of an array discharging. For example, many events are recorded by the TPM even when no biasing of the arrays is being performed and transient electric fields can be produced as systems are switched on or off during normal spacecraft operation. For the purposes of this mission it is, therefore, important to distinguish those signals which are caused by array arcing from those signals which are the result of normal spacecraft operation.

This section presents a statistical study of the properties of all signals recorded by the TPM from launch until the end of 1994. We will show that the analysis of the pulse shape may be used to distinguish transient electric fields resulting from discharges from other more benign causes.

We will use the term “spectral shape” to describe relationships between the measured parameters (unless otherwise noted, all “unit-less” TPM output values are in telemetry counts [0 to 255]) of the observed pulses as presented on a scatter plot. In this study we have concentrated on two characteristics: positive amplitude and the integral. Thus, very small pulses will have both small amplitude and integral values, whereas large short pulses will have a large peak amplitude but only a small integral value as a result of the short duration of the pulse. A small-amplitude, large-integral pulse may result from either a very broad small pulse or from a “ringing” pulse such that the integral value is large because of the train of small-amplitude excursions. Using these characteristics we have divided the recorded TPM signals into three categories:

1. Low amplitude–low integral pulses of ambiguous origin
2. Emitter-related noise characterized by pulses that are distributed approximately normally around an average integral value of approximately 79 ( $\approx 18$  nV-s) and an average positive amplitude of approximately 31 ( $\approx 8.9$  mV)
3. Discharges having integral values greater than 96 (28 nV-s) and increasing with increasing amplitude whose source is presumably the biased arrays.

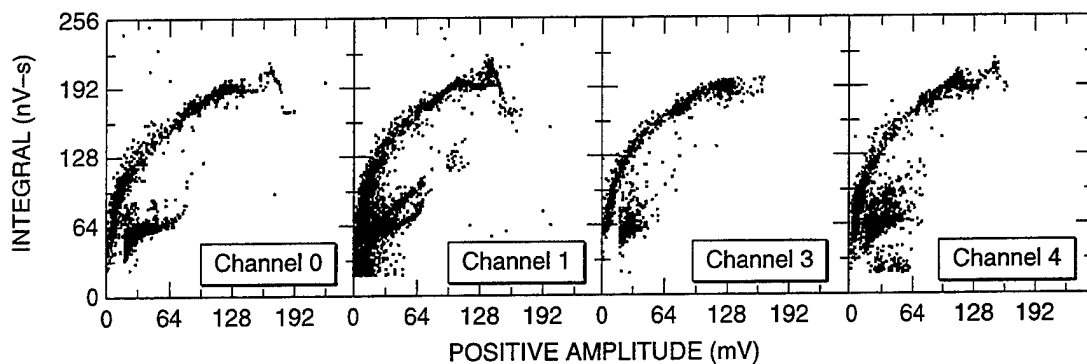
These categorizations were not made a priori. They are the result of statistical correlation of pulses in regions of integral–amplitude space.

The existence of category 1 simply indicates that there are often low-count signatures recorded by the TPM. Included in this category were signatures typically having values for amplitude and integral parameters that are less than 48 in instrument units, corresponding to values less than 14 mV for the amplitude and 8.9 nV-s for the integral. For these small pulses there does not appear to be any correlation between the amplitude and integral. It is difficult to determine the origin of these signals. The lack of substantial numbers of category 1 signals during intervals when the arrays were not being biased would tend to indicate that these signals result from the generation or application of the bias voltage. These small signals are present even during intervals of elevated voltage bias (e.g., when the voltage bias is  $> 300$  V negative). One might expect real discharges to increase in energy (and thus integral and amplitude) with increasing applied voltage. However, since there is no clear correlation with bias voltage and no correlation between amplitude and integral, the origin of these small signals remains ambiguous.

Category 2 is made up of the electric field noise observed when the emitter is on. In instrument units these pulses are distributed approximately normally about a mean integral of 79 (18 nV-s) and a mean amplitude of 31 (8.9 mV). Although not shown in this report, it is clear that these pulses are associated with the emitter. The emitter was operated only during intervals of positive biasing. Since this work is primarily focused on the characteristics of pulses during intervals of negative biasing, this category of pulses will not affect our data.

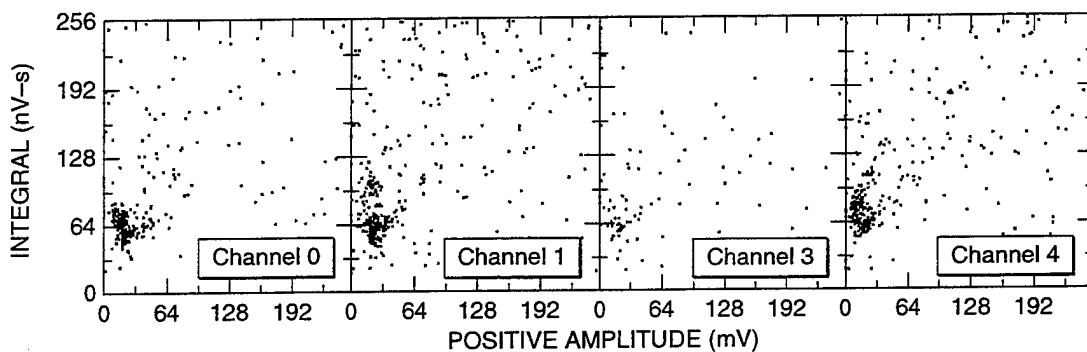
Figures 1 and 2 show data during times when the biasing was active and not active, respectively. Note the difference in the scatter plots of the two figures. During intervals when there was no biasing of the arrays, the recorded spectral shapes appear almost random. In contrast, the “spectral shapes” recorded during times when the arrays were being biased appear to have a consistent relationship between the integral and amplitude measurements. The integral increases with amplitude and eventually plateaus at a value of approximately 192 (280 nV-s).





4651fr/f1

**Figure 1. PULSE INTEGRAL vs. POSITIVE AMPLITUDE MEASURED BY THE FOUR TPM DETECTORS FOR ALL TIMES FROM 94215 TO 94309 WHEN BIASING WAS ACTIVE.**



4651fr/f2

**Figure 2. SIMILAR TO FIGURE 1, EXCEPT THE DATA HAVE BEEN RESTRICTED TO INTERVALS WHEN NONE OF THE ARRAYS WAS BIASED.**

The dividing line between these signals and others was determined by inspection. The dividing line is given by the following relationship:

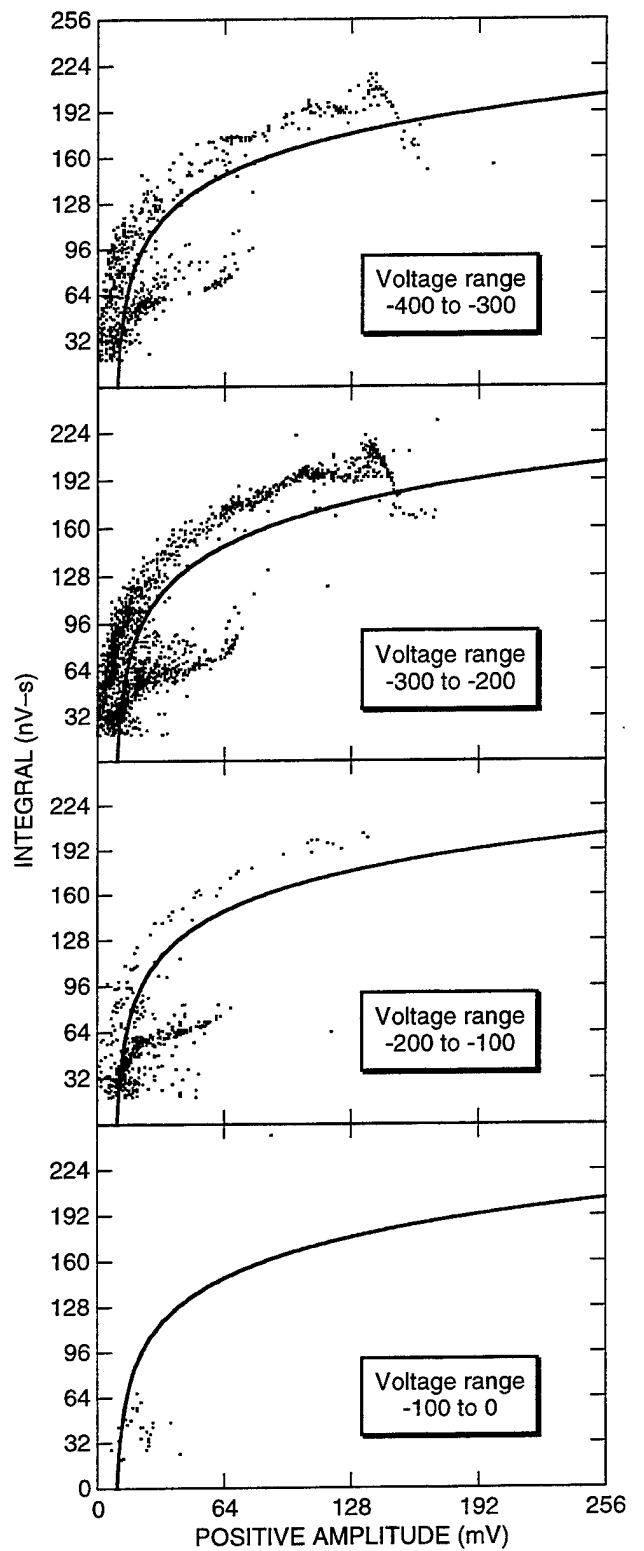
$$I = 37 \ln (A - 9) , \quad (1)$$

where  $A$  is the positive amplitude measured in instrument units, and  $I$  is the integral of the signal above which pulses are assumed to result from actual array discharges. The equation provides a convenient filter for determining which pulses are the result of discharges. For each pulse one would calculate the dividing integral from Eq. (1). If the recorded integral was greater than the integral given in Eq. (1), then the pulse would be recorded as a true discharge. Additionally, one should apply a restriction to remove the ambiguous small amplitude small integral cases discussed above. These could be removed by restricting the data to pulses in which the integral is greater than 48 ( $\approx 8.9$  nV-s).

Equation (1) also excludes the data centered on integral values of 64 ( $\approx 14$  nV-s) and positive amplitudes of 31 ( $\approx 8.9$  mV). They appear to be present even when the arrays are not biased, as seen in Figure 2. We, therefore, conclude that these events are probably not the result of real discharges.

Figure 3 shows integral versus amplitude scatter plots for four different ranges of negative biasing. The curve described by Eq. (1) is shown on each graph. One would expect that as larger potential differences are applied to the arrays, larger discharges would occur. These larger discharges would result in larger values of both the integral and the amplitude. Figure 3 shows that this is, in fact, the case. Those signals above the curve (i.e., for a specific amplitude those pulses that have an integral value greater than that given by Eq. (1) have higher integral and amplitude values at the highest voltages. In contrast, the signals below the curve have approximately the same spectral values during all bias conditions. This correlation between the strength of the signal and the applied voltage for signals below the curve and the lack of such a correlation for signals above the curve supports the use of Eq. (1) as a discriminator of real discharges.

**Discussion and Conclusions.** The operation of spacecraft will generate transient electric fields. These transient electric fields will be detected by the TPM even though they are not related to arc discharging. By analyzing the data from the PASP Plus mission we have determined an algorithm to distinguish real arc discharges from unrelated spacecraft noise. The algorithm was developed by analyzing the spectral shapes recorded by the TPM instruments



**Figure 3. PULSE INTEGRAL vs. POSITIVE AMPLITUDE MEASURED BY SENSOR 1 FOR FOUR DIFFERENT RANGES OF NEGATIVE BIASING [the curve described by Eq. (1) is shown on each graph].**

under various conditions and removing low-amplitude noise and emitter-induced signals. We have presented an algorithm which may be used to filter the TPM data to include only pulses resulting from discharges. As evidence that this filter successfully works, we have shown that the discharges predicted by the filter are more energetic at the higher bias voltages, as one would expect from an actual discharge.

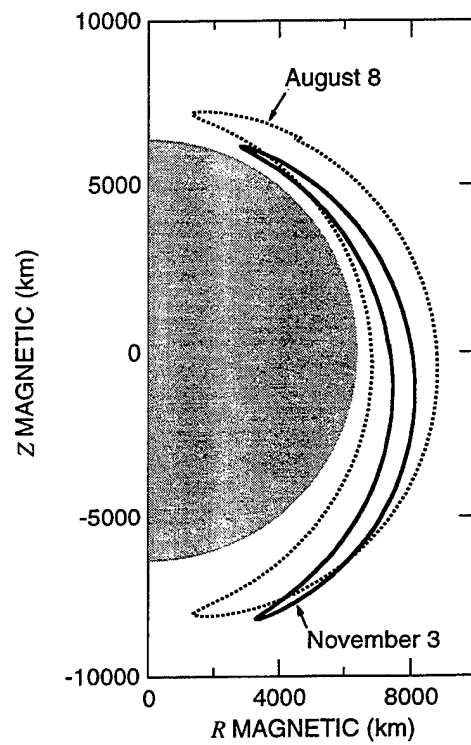
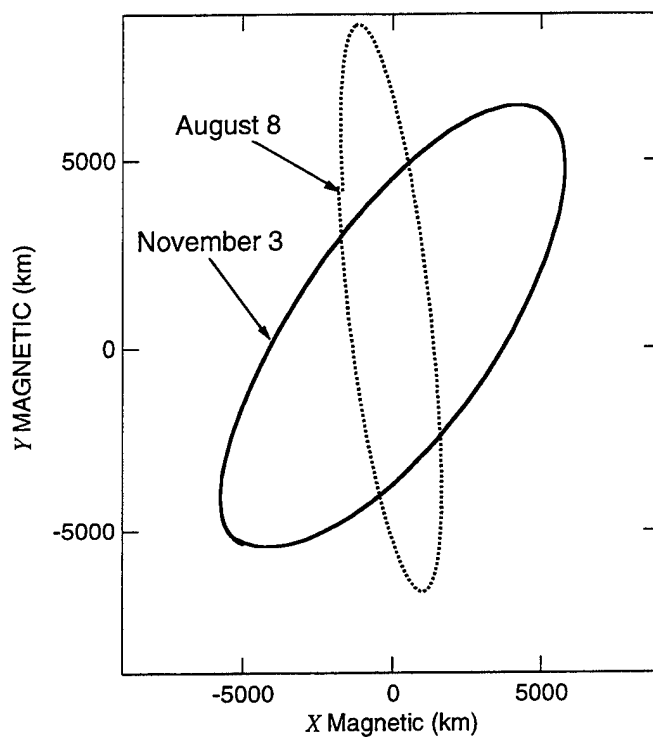
We have been unable to characterize signals with integrals that are less than approximately 48 counts. The lack of a consistent spectral shape for these signals may indicate that this signal is noise. If these low-amplitude signals are the result of discharges, the strength of the discharge is relatively small. A value of 48 counts for the integral is only 8.9 nV-s.

## **2.2 EFFECT OF THE LOCAL ENVIRONMENT ON DISCHARGES**

In Section 2.1, we showed that Eq. (1) could be used to identify real discharges from those resulting from the normal electrical noise associated with the spacecraft. In this section, we discuss how we have used Eq. (1) to identify when real discharges occur under various conditions. A "condition" here may be a particular voltage step, density, or time interval when a particular array is being biased. We count the number of 1-second TPM measurements made during a given condition. At each measurement point we use Eq. (1) to determine if a discharge occurred. As an additional limitation we require real discharges to have integral values larger than 48 in instrument units. The ratio of the number of real discharges recorded to the number of measurements made for a particular environmental condition yields the probability of discharge for that particular condition. We require at least 1000 measurements for a particular condition. Using this method we look at the effect of bias voltage on probability of discharge individually for each array. We then look at the combined effects of density and bias voltage on the probability of discharge.

The spacecraft orbital period is just under 2 hours. Figure 4 shows two typical orbits in magnetic coordinates. The x-axis lies in the magnetic equatorial plane and points toward the sun and the z-axis is aligned with the magnetic pole and is positive northwards. The y-axis lies in the magnetic equatorial plane and is defined such that the xyz coordinate system is right-handed. In a single orbit the spacecraft traverses a wide range in both magnetic local time and magnetic latitude. The spacecraft altitude varies within the orbit from approximately 360 to 2600 km. With such an orbit the density may vary over a large range. In this section, we examine the combined effect of density and bias voltage on the probability of discharge of Module 2.

Finally, we examine the effect of bias voltage on the size of the discharge rather than the probability. That is, given that a discharge has occurred, under what conditions is the discharge



4651fr/t4

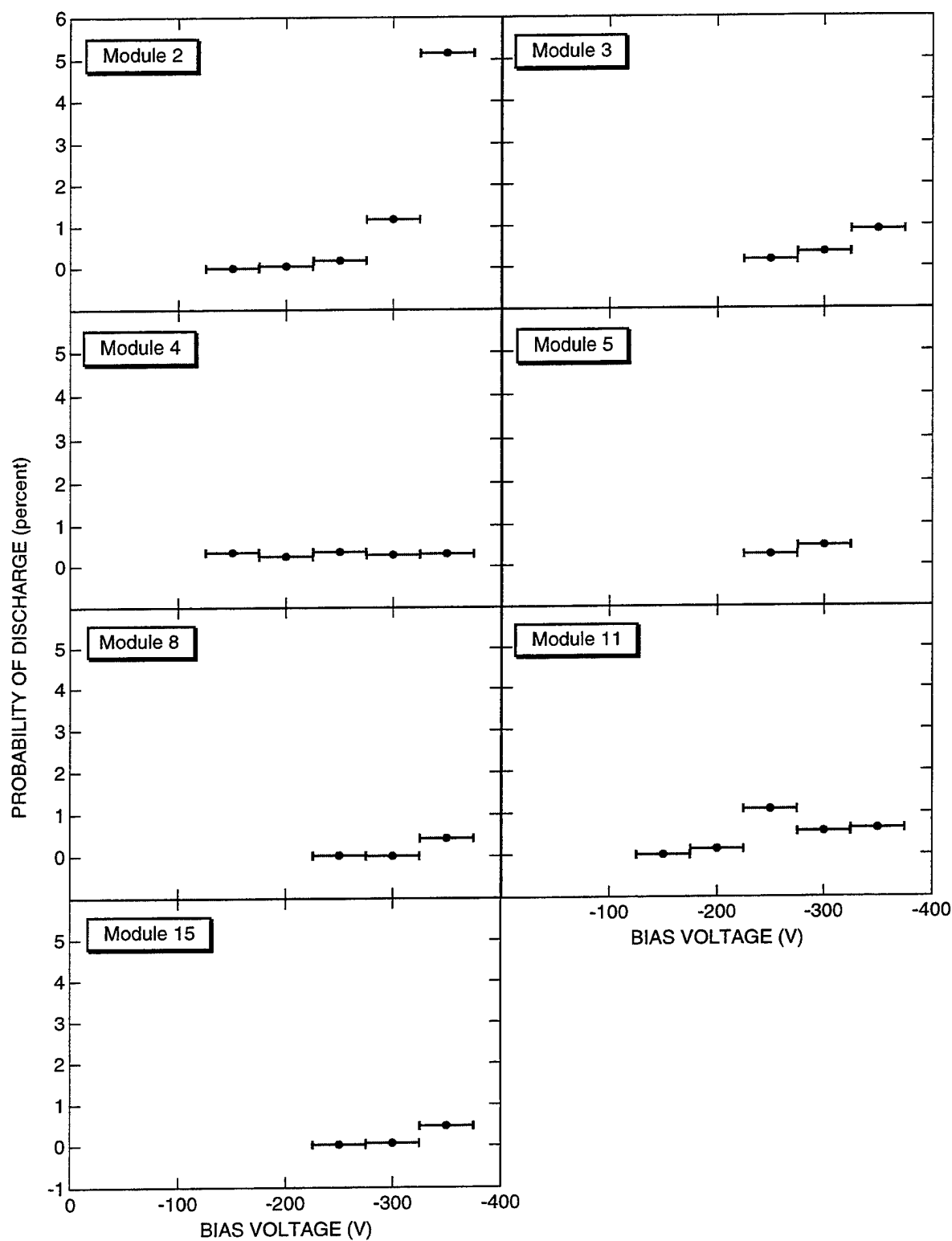
**Figure 4. TRAJECTORY OF THE SPACECRAFT FOR TWO ORBITS IN MAGNETIC COORDINATES (the coordinate system is defined in the text).**

likely to be large and thus potentially damaging to the spacecraft? Because the signal will decrease with distance, the size of the discharge recorded will depend on where the discharge occurred relative to the detector. Ideally, one would like to have a detector very close to the discharge site so the true amplitude of the discharge can be recorded. In this study, the maximum value recorded by one of the four detectors was used to create the statistical database of amplitude and integral measurements. This minimizes but does not eliminate the effect of distance on the recorded amplitudes. Thus, one can expect some amount of scatter in the results.

In Figure 5 we show the probability of discharge versus bias voltage for seven modules in seven representative arrays. Table 1 describes each of these seven arrays. The arc rate has already been shown to depend on the array temperature with more discharges occurring during eclipse intervals (Soldi and Hastings, 1995). Since the arrays could always be artificially heated to avoid these cold temperature discharges, as suggested by Soldi and Hastings (1995), we have restricted the data in Figure 5 to non-eclipse intervals. Thus, this figure represents discharge rates, including the cases where such heating of the arrays was implemented. It is clear that the standard silicon array (Module 2) is the most likely array to discharge. These discharges are more likely to occur at voltages above  $-275\text{V}$ . Array/Module 3 shows only very modest discharging at voltages above  $325\text{V}$ . The other arrays show almost no propensity to discharge in non-eclipse regions.

**Table 1: ARRAY TYPE AND ASSOCIATED MODULE NUMBER**

Module No.	Array Type
2	Si (Std)
3	Si (wrap-through connectors)
4	GaAs/Ge 3.5 mil
5	Si (APSA)
8	GaAs/Ge (wrap-through connectors)
11	GaAs/Ge 7 mil
15	GaAs/GaSb mini-dome



4651fr/f5

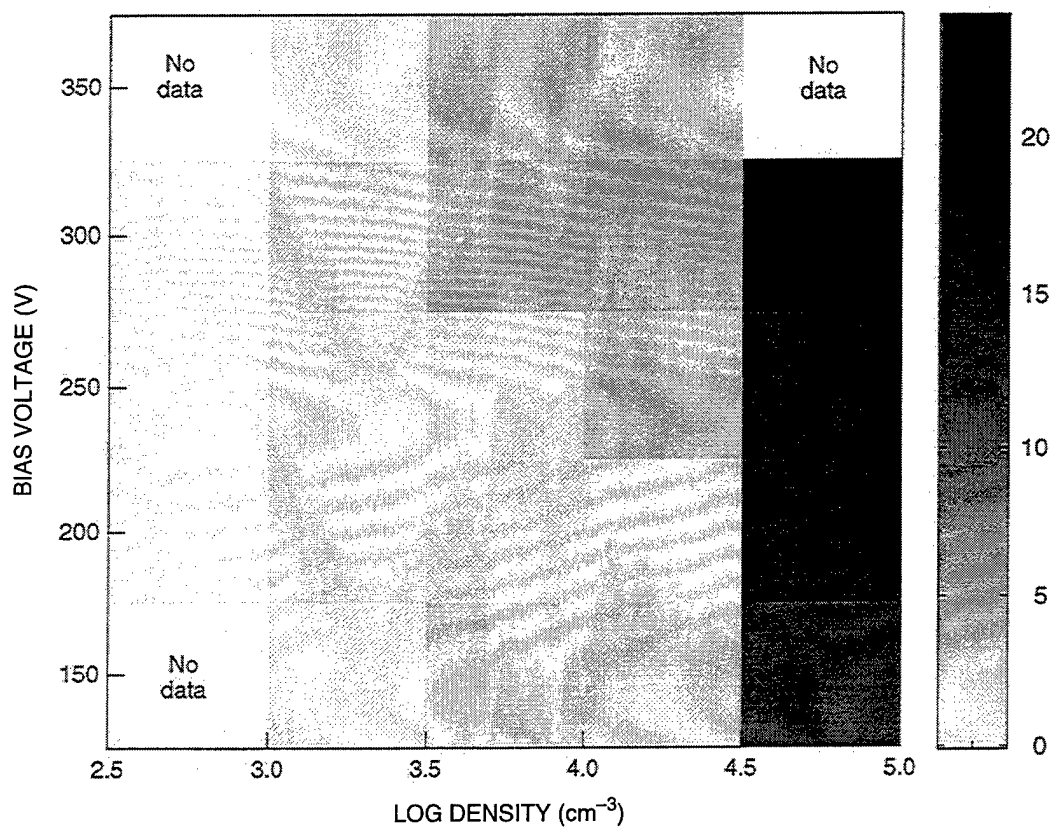
Figure 5. PROBABILITY OF DISCHARGE vs. BIAS VOLTAGE DURING NONECLIPSE INTERVALS FOR THE MODULES LISTED IN TABLE 1 (horizontal array bars show the width of the voltage bin).

Figure 6 shows the probability of discharge for Module 2 during the three negative biasing intervals from 94215 to 94309 including the eclipse intervals. The data have been binned into intervals of constant bias voltage and density. The color intensity shows the probability of discharge. White indicates that no data were present in that particular voltage-density bin. The figure shows that, for a given density, the probability of discharge increases with increasing voltage. This agrees with the result shown in Figure 5. However, Figure 6 additionally shows that, for a fixed bias voltage, the probability of discharge increases with increasing density, with the maximum probability of discharge occurring during intervals of large density and large negative biasing. Thus, even during times when the bias voltage is small the array may discharge if the surrounding density is large.

As in the above, most prior studies have concentrated on parameterizing the arc rate with various parameters—for instance, the correlation between increased arc rates and energetic electron injections shown by Shaw et al. (1976) or the modeled local time dependence of arcing rate for Space Station Freedom given by Hastings et al. (1992). The TPM provides much more information than just arc rate. The shape of the discharge pulse is also recorded. In the previous sections we have shown that a wide range of pulse shapes is possible during discharges. Some may be relatively small while others may involve larger voltages. For example, Figure 3 shows that it is not uncommon during high-voltage biasing to observe pulses with integral values of 200 and amplitudes of 144. These values represent measured pulses of 360 nV-s and 0.130 V. Since these voltages represent the values measured at the sensor and the signal strength diminishes with distance traveled, the voltages measured at the source would be much higher. These large discharges are more likely to affect the spacecraft electronics. Most prior studies have not distinguished these potentially more harmful discharges from the smaller, more numerous ones. In Figure 7, we show that the size of the discharge and not just the arc rate is proportional to the bias voltage. The figure shows the average positive amplitude and integral of discharges during negative biasing intervals of array 2. The large discharges occur at the higher bias voltages. Thus, if a discharge does occur, the discharge is more likely to be large and thus possibly immediately harmful to spacecraft conditions if the bias voltage is large.

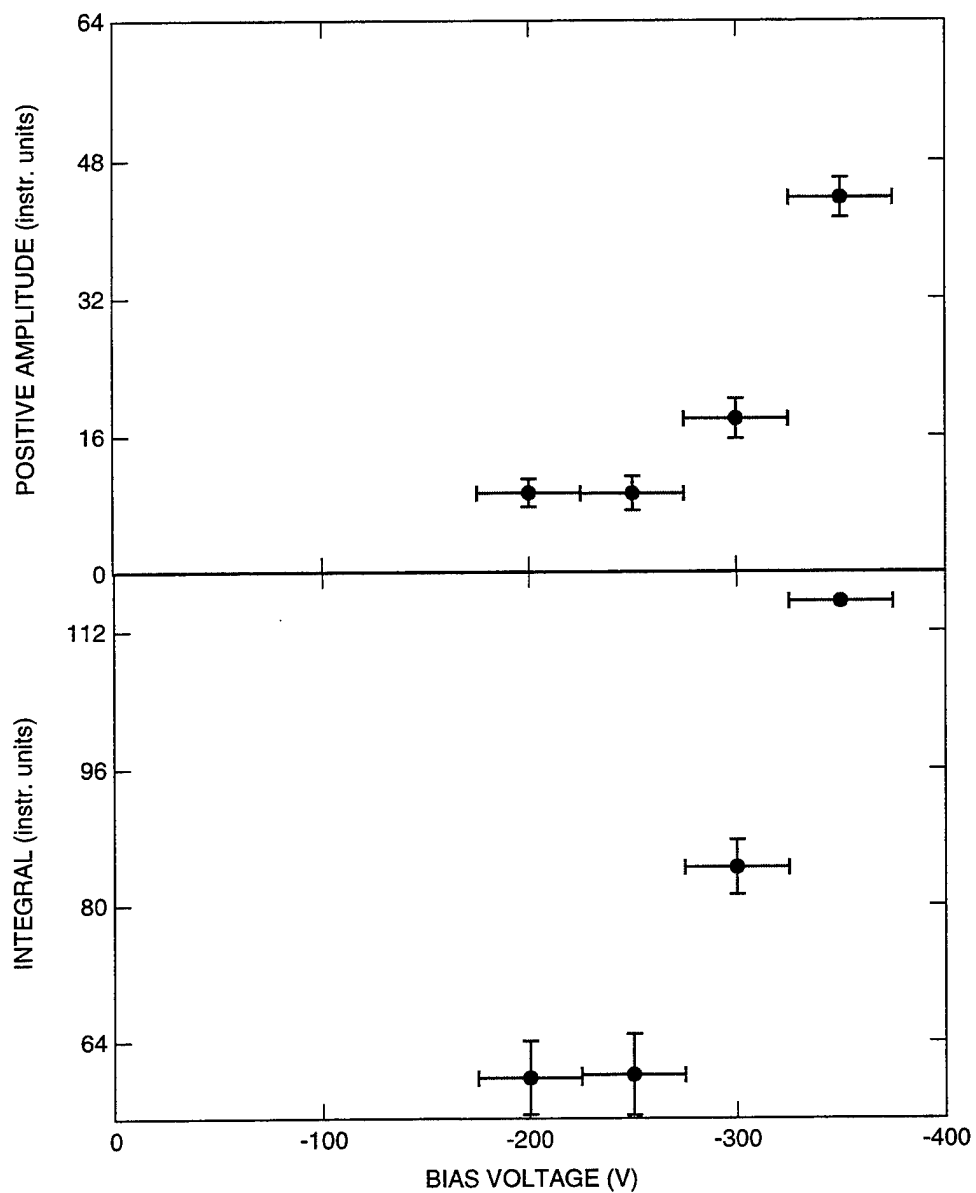
**Discussion and Conclusions.** The analysis shown here is similar to portions of the analysis done by Soldi and Hastings (1995). However, we have identified real discharges from background electrical noise by using the filter described within this section. This filter is based on the amplitude and integral of the pulse as determined from analyzing the grouping of discharges in amplitude–integral space. In this manner, we can identify real discharges with no a priori decisions about under what conditions they are likely to occur.





4651fr/f6

**Figure 6. PROBABILITY OF DISCHARGE FOR MODULE 2 AT VARIOUS NEGATIVE BIAS VOLTAGES AND ELECTRON DENSITIES AS MEASURED BY THE LANGMUIR PROBE (white indicates no data in that particular bin).**



4651fr/f7

**Figure 7. POSITIVE AMPLITUDE AND INTEGRAL vs. BIAS VOLTAGE FOR MODULE 2 DURING NONECLIPSE INTERVALS (horizontal error bars show the width of the voltage bin; vertical error bars show the standard error of the measurement).**

The results presented here are in general agreement with the work of Soldi and Hastings. With the exception of the standard silicon array (Module 2), all of the arrays shown in Table 1 showed a very low propensity to discharge during non-eclipse intervals. In particular, the mini-dome array (Module 15) had a very low probability of arcing due to the shielding introduced by the dome. Of the arrays shown in Table 1, Module 2 of the standard silicon array had the largest propensity to discharge. During non-eclipse intervals the probability of discharge increased at voltage beyond  $-275\text{V}$ . However, as seen in Figure 6 the ambient density can lower the voltage at which discharging occurs.

We have also shown that the size of the discharge increases with increasing bias voltage. Although it may seem obvious that when large potentials are present larger discharges may result, we are not aware of prior results showing this effect. This effect means that not only will larger voltages make discharges more likely, but when discharges do occur they are more likely to be large discharges. A similar result was shown earlier in this section during the description of the creation of the filter. However, it should be noted that the filter used here was developed based on the correlation between the integral and amplitude measurements seen in Figure 1, rather than any dependence on bias voltage.

### **2.3 LOCATION OF DISCHARGES**

The TPM instrumentation consists of four detectors on the spacecraft plus a current sensor. Three of the detectors (Numbers 0, 3, and 4) are on the body of the spacecraft while the fourth (Number 1) is located on the solar panel. With such a configuration and with a discharge strong enough to be seen in at least two detectors, it is theoretically possible to determine the location of any discharge that occurs on the spacecraft.

Before launch the detectors were calibrated by using a static discharge at various locations around the spacecraft and recording the signal in each of the four detectors. Thus, the response of each detector is known for a single fixed transient electric field occurring on a grid that approximately covers the entire spacecraft. Using this knowledge of the response of the detectors, Adamo et al. (1994) showed it was possible to apply the same fixed transient electric field at a given location, and use a least squares minimization to determine where the discharge occurred. In space, however, the situation is more complicated. One is not sure a priori what the size of the discharge is. There are other transient fields present that were not present in the clean room environment used by Adamo et al., and the propagation of the transient signals may be modified by the local plasma environment invalidating the ground calibrations. In addition, during an actual discharge electrons are blown directly off the surface. The propagation from this "antenna" may be quite different from that of the spark generator described in Adamo et al.

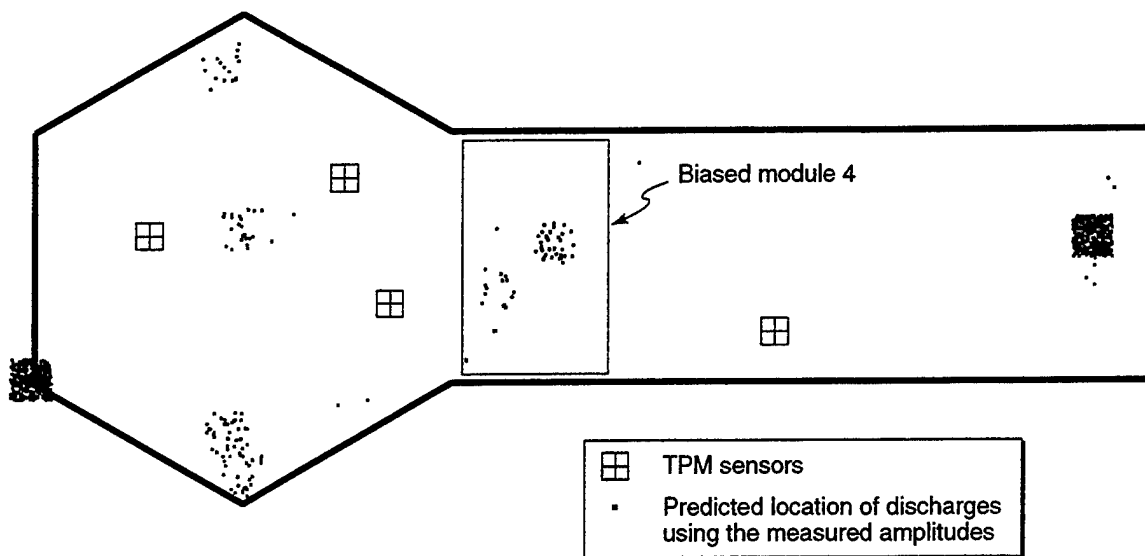
Thus, the source of the transient fields may have different characteristics in space than on the ground.

We have tried several methods to try to find the location of discharges recorded by the TPM. We have used a least squares minimization technique similar to that used by Adamo et al. (1994) to find the location at which the discharges occur. Figure 8 shows the predicted locations of the discharges for intervals when Module 4 was being biased. Only intervals of negative biasing were examined. The events were restricted to real discharges using the restriction algorithm described above. Additionally, the data were limited to large discharges where the integral value was above 48 in instrument units. The figure shows that the preponderance of the predicted locations does not appear to be near the biased array. Similarly scattered results are obtained during the biasing of the other arrays.

In Figure 8, the amplitude of the signal recorded by each sensor was compared to the calibrated response of the sensors to a known signal at a known location. Amplitude was chosen because in the ground calibration, amplitude was determined to yield the least variation in predicted location (Adamo et al., 1994). As we have seen in Section 2.2, real discharges have a characteristic relationship between the integral and amplitude. In an attempt to improve the results shown in Figure 8, we have modified our minimization technique to minimize the difference in both the measured amplitude and integral with the calibration measurements of amplitude and integral. The location on the spacecraft that produced a minimum in this difference was chosen as the predicted location of the discharge. Figure 9 shows the result of this technique when Module 4 was being biased. Over 90% of the predicted locations occur in or very near to Module 4.

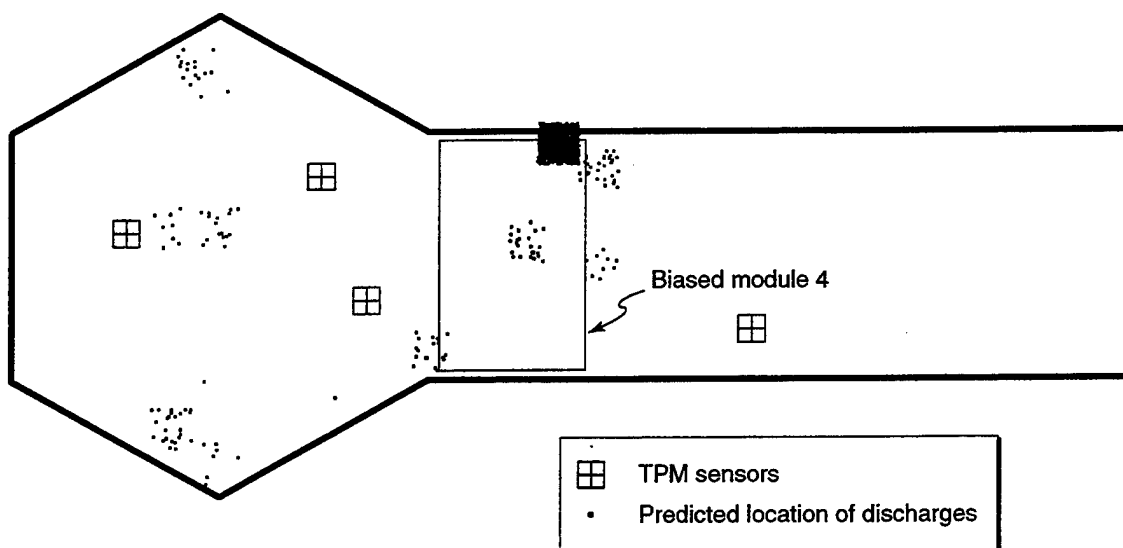
However, the success shown in Figure 9 is fortuitous. Figure 10 shows the same technique used in Figure 9 applied to intervals when Module 3 was being biased. Note the similarity in predicted points. The points surrounding Module 4 appear to be minimums in the response functions generated in the ground test. Thus, the use of both the amplitude and integral in determining the location of the discharge is not successful.

In the above analysis method we have used the response functions for the instruments generated on the ground using a hand-held electric field stimulus device. Such a device should produce fairly consistent signals. The discharges in space may, of course, have quite different initial spectral shapes than those produced by the device. The initial amplitude of the discharge can be added as a free parameter in the minimization routine. In Figure 11 we show the results of this method when Module 4 was being biased. The same restrictions on the data used in Figure 8 were applied to the data. Some of the predicted locations of the discharges do fall



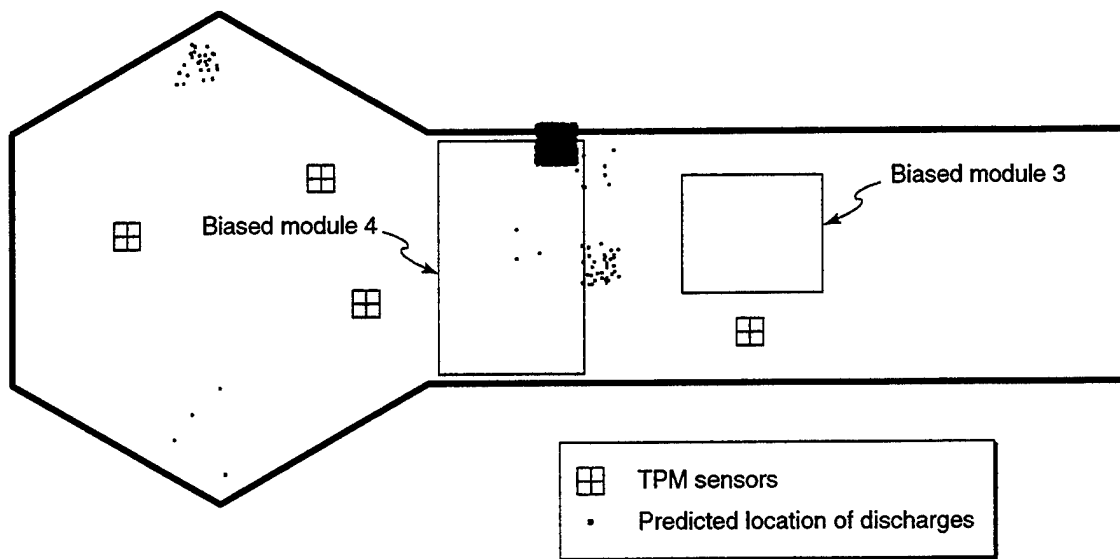
4651fr/18

**Figure 8. TOP VIEW OF THE SPACECRAFT WHERE THE POSITION OF THE BIASED MODULE AND THE LOCATION OF THE FOUR TPM SENSORS ARE SHOWN.**



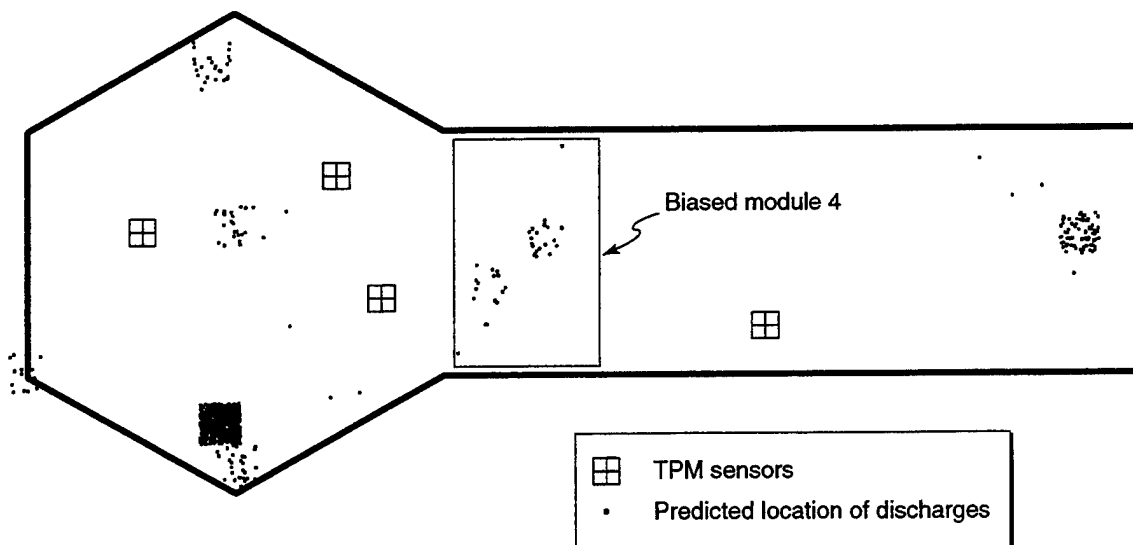
4651fr/19

**Figure 9. SIMILAR TO FIGURE 8, EXCEPT BOTH THE AMPLITUDE AND INTEGRAL WERE USED TO FIND THE PREDICTED LOCATION OF THE DISCHARGE.**



4651fr/f10

**Figure 10. SAME AS FIGURE 9, EXCEPT FOR INTERVALS WHEN MODULE 3 WAS NEGATIVELY BIASED.**



4651fr/f11

**Figure 11. SIMILAR TO FIGURE 8, EXCEPT THE INITIAL AMPLITUDE OF THE SIGNAL WAS TREATED AS A FREE PARAMETER DURING THE MINIMIZATION ROUTINE TO FIND THE PREDICTED LOCATION OF THE DISCHARGE.**

within Module 4, but most of the predicted locations do not appear to be near the biased module. Although not shown here, similar results were obtained with this method when the other modules were biased.

**Discussion and Conclusions.** During prelaunch calibrations, it was shown that the location of an artificially induced transient electric field could be predicted using the TPM sensors (Adamo et al., 1994). We have used three different techniques in an attempt to duplicate these results for real discharges occurring in the space environment. We have used both the measured amplitude and amplitude and integral to compare with the ground-calibration data. Neither of the two methods was totally successful as seen in Figures 8 and 9. We have also included the initial amplitude of the signal as a free-fitted parameter in the minimization routine. This method was also not completely successful as shown in Figure 11. Of the three techniques, using both the amplitude and the integral of the discharge in determining the location of the discharge was the most successful.

At first glance, it is surprising that the results obtained on the ground could not be repeated during the mission. However, conditions during flight are quite different from those in the clean room. During an actual discharge an arc occurs between two parts of the spacecraft. During the ground calibration this could not be done. Instead, an arc was created between two plates with the lower ground plane separated from the spacecraft surface by a thin dielectric (e.g., clean room cloth or writing paper). The propagation of such a wave may be different from that generated by a discharge on the surface of the spacecraft. Thus, the response functions generated on the ground may not be applicable to the case of an actual discharge occurring during the mission.

## 2.4 SUMMARY

In addition to measuring the number of pulses, the TPM records the maximum integral, positive and negative amplitude, and derivative information of the pulse during the counting interval. We have used this information about the shape of the pulse to identify those pulses associated with discharges from those associated with more benign electrical noise. We have shown that pulses filtered by this method occur predominately during large negative voltages, supporting the assertion that this filter restricts the data to discharge-related pulses.

We believe the use of integral and amplitude to determine true discharges to be relatively unique. Before this study there was no a priori reason to believe that spacecraft discharge pulses would have a characteristic amplitude-integral relationship. Although not discussed in this report, it is interesting that pulses associated with emitter operation have their own different

amplitude–integral relationship. These results suggest many sources of electrical noise on the spacecraft may be identified by the relationship of the pulse parameters.

The use of multiple TPM sensors to determine the location of a discharge was not entirely successful. Of the three techniques used in this study, using both the amplitude and the integral of the discharge in determining the location of the discharge was the most successful. It is likely that the propagation of waves in the space environment is quite different from that of the clean room where such a technique was successfully implemented.

As expected, the probability of discharge was shown to increase with increasing bias voltage. Of the arrays listed in Table 1, only Module 2 and Module 1 (not discussed in this report) of the standard silicon array showed a relatively large propensity to discharge during non-eclipse intervals. Additionally, the size of the discharge increases with increasing bias voltage. This result is new since previous studies have concentrated only on discharge rates. Thus, as larger voltages are used, not only are discharges more likely to occur, but they are more likely to be large damaging discharges.

A final comment should be made on the applicability of the results presented in this section. In almost all instances of this study, the data have been restricted to intervals of negative biasing. From the results presented here, it is impossible to comment on the existence of discharges during positive biasing or on environmentally induced discharges not associated with the artificial biasing of the arrays. While the existence of this kind of discharging may not be intuitively obvious on the basis of present theories, this study can make no comment on this area. Although on average discharges are less likely during low-voltage conditions, it would be an error to interpret this study as supporting the idea that discharging cannot occur during low-bias voltages. Indeed, Figure 6 suggests that denser plasma environments may favor discharging at low-bias voltages.

### **3 REFERENCES**

- Adamo, R. C., K. L. Giori, and D. R. Dana, "PASP Plus Transient Pulse Monitor (TPM) - Preflight Characterization Report," PL-TR-94-2131, SRI International, Menlo Park, CA, January 1994, ADA282582.
- Dana, D. R., "Transient Pulse Monitor (TPM)," PL-TR-91-2131, SRI International, Menlo Park, CA, November 1991, ADA244502.



- Guidice, D., and K. Ray, "PASP Plus Measurements of Space Plasma and Radiation Interactions on Solar Arrays," paper AIAA 96-0926, 34th AIAA Aerospace Sciences Meeting, Reno, Nevada, January 1996.
- Hastings, D. E., M. Cho, and J. Wang, "The Space Station Freedom Structure Floating Potential and the Probability of Arcing," *J. Spacecr. Rockets*, 29, pp. 830-834, 1992.
- Shaw, R. R., J. E. Nanevich, and R. C. Adamo, "Observations of electrical discharges caused by differential satellite charging," in *Spacecraft Charging by Magnetospheric Plasmas*, ed. A. Rosen, American Institute of Aeronautics and Astronautics, New York, 1976.
- Soldi, J. D., and D. E. Hastings, "Arc Rate Simulation and Flight Data Analysis for the PASP Plus Experiment," PL-TR-95-2126, Massachusetts Institute of Technology, Cambridge, MA, September 1995, ADA301837.

## APPENDIX

### TPM HARDWARE DESCRIPTION

The Transient Pulse Monitor (TPM) developed under contract F19628-86-C-0231 detects and characterizes transient currents and electric fields on satellites for the purpose of studying electrostatic discharges. As a diagnostic tool for the Photovoltaic Array Space Power Plus Diagnostics (PASP Plus) experiment, which studies the long-term performance and environmental interactions of high-voltage solar arrays, the TPM measures the severity and frequency of discharges that may result from high-voltage operation. The TPM is also well-suited to measure discharges that may result from environmental interactions, unrelated to the high-voltage arrays, that are known to affect all spacecraft.

The TPM has two types of sensors: one that measures currents conducted on a wire, and another that measures electric fields. Both sensor types are optimized to measure pulses of a few nanoseconds to many microseconds in duration, which includes the range expected to result from spacecraft discharges. For the PASP-Plus experiment, the TPM has been configured with one current sensor and five electric-field sensors. The current sensor measures transients on the output of the high-voltage power supply that is used to bias the solar cells. The electric-field sensors are located near the solar cells to detect discharges in their vicinity. Only the results of the electric-field sensor measurements are discussed in this report.

The TPM characterizes pulses in a way fundamentally different from that of transient digitizers. It uses analog circuitry to derive key parameters of transients—peak amplitude, peak derivative, and integrated magnitude—in real time. This approach has several advantages over transient digitizers: The circuitry is more compact, consumes much less power, has wide dynamic range, and rivals the state of the art in bandwidth. Finally, it produces data that are almost immediately usable for engineering analysis of transient characteristics.

A complete description of the TPM hardware and related information can be found in the following project reports:

- Adamo, R. C., K. L. Giori, and D. R. Dana, "PASP Plus Transient Pulse Monitor (TPM) - Preflight Characterization Report," Scientific Report No. 1, PL-TR-94-2131, SRI International, Menlo Park, CA, January 1994, ADA282582.
- Dana, D. R., "Transient Pulse Monitor," Scientific Report No. 2, GL-TR-89-0305, SRI International, Menlo Park, CA, October 1989, ADA220353.
- Dana, D. R., "Flight Unit Information Report," Equipment Report, SRI International, Menlo Park, CA, November 1991.
- Dana, D. R., "Transient Pulse Monitor (TPM)," Final Report, PL-TR-91-2131, SRI International, Menlo Park, CA, November 1991, ADA244502.
- Dana, D. R., and J. S. Thayer, "Transient Pulse Monitor (TPM)—Ground Support Equipment," SRI International, Menlo Park, CA, December 1988.
- Thayer, J. S. , J. E. Nanevich, and D. R. Dana, "Transient Pulse Monitor," Scientific Report No. 1, AFGL-TR-88-0147, SRI International, Menlo Park, CA, May 1988, ADA201211.